Available online at www.sciencedirect.com

SCIENCE DIRECT®

Engineering Geology 75 (2004) 15–31

ENGINEERING GEOLOGY

www.elsevier.com/locate/enggeo

Bearing capacity of rock over mined cavities in Nottingham

A.C. Waltham[a,*], G.M. Swift[b,1]

[a] Civil Engineering Department, Nottingham Trent University, School for Property and Construction, Nottingham NG1 4BU, UK
[b] School of Chemical, Environmental and Mining Engineering, University of Nottingham, Nottingham NG7 2RD, UK

Received 18 December 2003; accepted 26 April 2004
Available online 17 June 2004

Abstract

A significant geohazard is created in Nottingham, UK, by hundreds of man-made caves cut in the weak sandstone beneath the city centre. Stability of the caves has been assessed by a single full-scale loading test, by numerical modelling with FLAC and by physical modelling in plaster. For typical caves 4 m wide, bearing capacity of the rock roof rises from 2 MPa where it is 1 m thick to 8 MPa where 3 m thick. Stability decreases over wider caves and where the loading pad edge is over the edge of the cave. Numerical modelling of a very wide cave revealed the failure mechanisms and also showed that an internal support wall increased roof bearing capacity by 50%. Local building regulations that require 3–5 m of rock cover over the sandstone caves appear to be conservative. In stronger rocks, including karstic limestone, a guideline that cover thickness exceeds 70% of the cave width appears to be appropriate.

Keywords: Geohazards; Cavities; Foundations; Bearing capacity; Sandstone; Numerical modelling

1. Introduction

Ground cavities are potential hazards for many construction projects, and the city of Nottingham is built on rock that contains many hundreds of mined voids. The city centre stands on a low hill of Triassic Sherwood Sandstone. This rock is of low strength, but has only widely spaced bedding planes and fractures, so that it has a relatively high rock mass strength. It is therefore easily excavated to create stable underground rooms, locally known as caves (even though they are entirely artificial). Well over 500 caves are known beneath the city (Walsby et al., 1990; Waltham, 1992).

The oldest caves date back about 1000 years, and nearly all pre-date 1900. With few exceptions, they were excavated to provide working or storage space within a growing and often over-crowded town. Most caves are 3–5 m wide, and up to 10 m long; many are individual rooms, while others are clusters of rooms reached from the foot of a single staircase tunnel. The rock over the caves is generally 1–4 m thick; they were excavated as sub-basements as close as possible beneath the conventional cellars that were sunk into the surface profile of soil and weathered sandstone. In the old part of town (now the centre),

* Corresponding author. Tel.: +44-115-981-3833.
E-mail addresses: tony@geophotos.co.uk (A.C. Waltham), g.m.swift@salford.ac.uk (G.M. Swift).
[1] Now at School of Science, Computing and Engineering, Salford University, Salford M5 4WT, UK.

0013-7952/$ - see front matter © 2004 Elsevier B.V. All rights reserved.
doi:10.1016/j.enggeo.2004.04.006

Fig. 1. A construction site in central Nottingham (seen from a tower crane) with 10 cellar caves unroofed when the ground profile was lowered by 1–2 m.

nearly every building has a cellar cave beneath it, with significant implications for site re-development (Fig. 1).

1.1. Strength of the sandstone

The sandstone in which the Nottingham caves have been excavated is a fine-grained material consisting almost entirely of sub-angular quartz grains bonded by clay particles that form bridges between the grains. It has a mean porosity of 17%, largely due to the dissolutional removal of an original calcite cement that is completely absent in all the rock at and near outcrop in which lie the caves.

Intact rock strength is closely related to the degree of weathering. Unconfined compressive strength (UCS) decreases from over 30 MPa at depths greater than 10 m to around 1 MPa close to rockhead (Waltham, 1993). The rockhead is not clearly defined, as the rock progressively disintegrates into an in situ dense sand. At nearly all sites, the weathered rock and sand were removed to place conventional basements, and the caves lie beneath in rock that has UCS >3 MPa. Strength properties for the intact sandstone, listed in Table 1, are based on numerous uniaxial compression tests on dry material (Forster, 1989; Waltham, 1993), with the friction angle and cohesion derived from a modified Hoek–Brown failure envelope for analytical input.

The sandstone loses strength when it is saturated, but recovers when it is subsequently dried. The caves are normally dry as they lie beneath buildings; accidental water input is the main cause of roof failure leading to crown hole collapses (Waltham, 1993). When damp, the sandstone loses only about 15% of its dry strength.

The Sherwood Sandstone originated as alluvial fans. It is generally of massive appearance, but flood events created horizons rich in pebbles and mud flakes that form bedding plane weaknesses 1–5 m apart. Many intervening beds have poorly defined cross bedding. In a cave roof invaded by a water leak, the visually homogeneous rock is saturated and placed in tension for a long period; when it fails, it splits into beds only 10–40 mm thick. This hidden heterogeneity accounts for anisotropy in the strength parameters. Compressive strength declines by 20% when orientated cube samples are loaded parallel to the bedding, though they still fail in the conventional shear pattern, and

Table 1
Measured strength properties of sandstone in Nottingham

Material	Nottingham Sandstone	Commerce Square Sandstone	Wollaton Street Sandstone
Compressive strength (UCS), MPa	4.12–10.31	22.7–33.1	3.3
Tensile strength (UTS), MPa	0.35–0.75	1.06–1.54	0.34–0.50
Young's modulus, GPa	1.2	2.2	1.2
Poisson's ratio	0.25	0.25	0.25
Unit weight, kN/m^3	23	23	23
Friction angle, °	69	61	33
Cohesion (shear strength), MPa	0.94	2.95	1.10

Nottingham Sandstone is typical material from the Sherwood Sandstone in the area. Commerce Square Sandstone is rock collected from the site of the cave loading test after failure. Wollaton Street Sandstone is rock collected from the fallen roof slab in the cave beneath the road.

tensile strength declines by nearly 40%. It is significant that laminations are not normally detectable in weathered, cut or fractured faces of the sandstone; the rock mass strength is therefore significantly lower than it appears to be from any conventional visual assessment.

1.2. Cave roof testing

Research into the bearing capacity of cave roofs in the Nottingham Sandstone has followed three lines in parallel. A single cave roof was loaded to failure, but further sites have not been available for destructive testing. Numerical modelling was first based on three-dimensional finite element analysis; planar weaknesses could not be adequately built into the model, and real failure criteria were only established after a rock mass factor of about 0.1 was introduced to represent random fractures (Roodbaraky et al., 1994). Subsequent use of finite difference modelling has proved more successful, though it has to date been restricted to two-dimensional profiles (Swift et al., 2000). Physical models have demonstrated the failure mechanisms, but could not adequately simulate the micro-fracture weaknesses that reduce the rock mass strength.

2. Test loading of a sandstone cave roof

Re-development of a site in Commerce Square, in central Nottingham, provided the opportunity for a full-scale test loading of a cave roof to failure. Within a complex cave system, two superimposed caves were separated by an unusually thin rock shelf that was just 0.5 m thick (Fig. 2). For practical reasons, this was loaded from below, by hydraulic jacks bearing upwards onto a pad 400 mm^2 (Fig. 3A). The width of the upper cave was 4 m, and site conditions determined an off-centred loading. After failure, blocks of sandstone were removed to determine their strength parameters (Table 1). The rock at the test site is significantly stronger than the sandstone in which most of the other caves have been excavated. This is because it is much less weathered at a depth of 10 m below rockhead; the cave is reached through a horizontal tunnel into the foot of a nearby cliff, and its depth is therefore not typical.

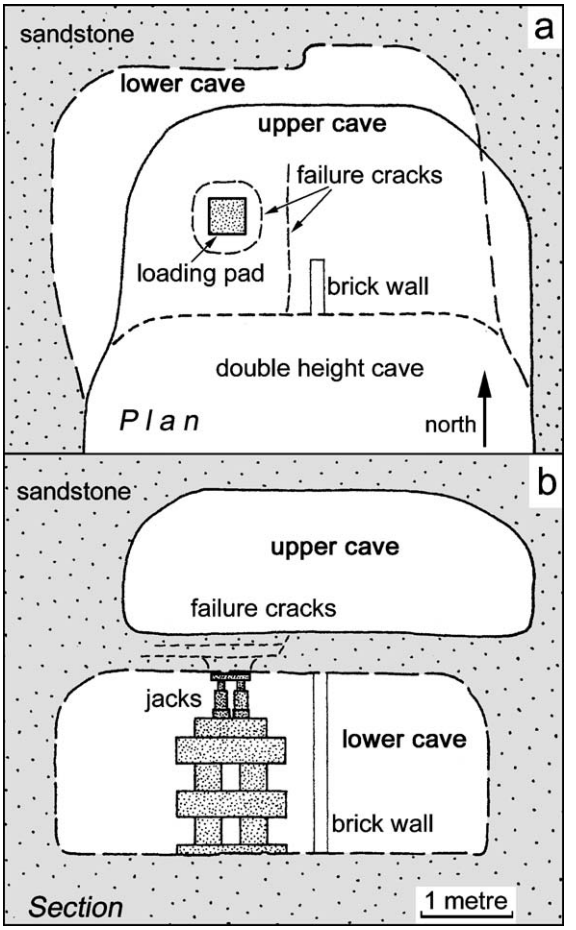

Fig. 2. Plan (a) and section (b) of the cave under Commerce Square containing the sandstone shelf that was test loaded to failure.

As the cave roof was loaded, the sandstone split into three beds of roughly equal thickness (Fig. 3B). The intervening bedding planes had been identifiable along the broken edge of the rock shelf prior to the test loading. Deformation continued until the bearing pad had been displaced 25 mm, when failure occurred at a maximum loading of 340 kN. Dismembering of the broken rock revealed that the lower bed, in contact with the bearing pad, had failed in a flared plug (Fig. 3C). This had spread the load onto the subsequent (higher) beds, which had fractured in cantilever, initially along a fracture 400 mm from the edge of the bearing pad that may have been a pre-existing weakness in the rock. Exposed fractures that were oblique through the sandstone showed stepped profiles that picked out minor

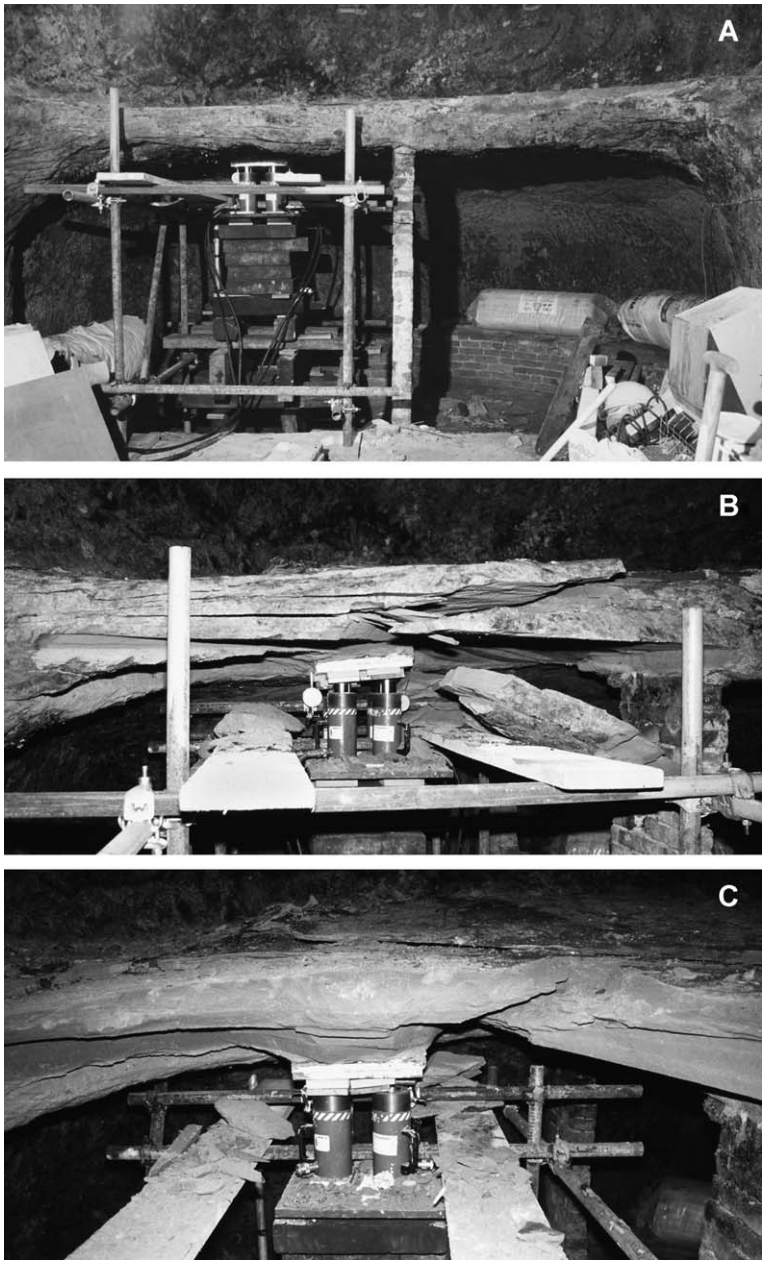

Fig. 3. The sandstone shelf in the Commerce Square cave before and after loading to failure. (A) The loading rig in place, with the jacks ready to impose upward stress. (B) The sandstone after failure, with opened bedding planes, some oblique fractures and some fallen slabs. (C) The sandstone after failure, with loose material removed to expose the flared plug through the bed against the loading pad.

bedding planes at intervals of about 30 mm. Neither these laminations nor any possible fracture that initiated the failure across the beds was visible before the sandstone was deformed by the test loading.

Though the very small rock thickness loaded in this test hindered direct interpolation to the bearing capacity of typical and much thicker cave roofs, the data was critical for the creation of a realistic numer-

ical model and also for calibration of the physical models.

3. Numerical modelling of the sandstone caves

The caves were modelled using Fast Lagrangian Analysis of Continua (FLAC), a two-dimensional finite difference code (Itasca, 1995). In FLAC, algebraic equations are solved using dynamic relaxation. This is an explicit time-marching procedure where the dynamic equations of motion are integrated step by step. Static solutions are created by employing damping terms within these equations, to remove kinetic energy from the system under observation. As a convergence criterion, FLAC employs the nodal unbalanced force—the sum of forces acting on a node from its neighbouring elements; at a node in equilibrium, these forces sum to zero. Elements within the finite difference grid were only 0.1 m across around the cave, and increased in size towards the model boundaries, which were at least two cave diameters from the cave and therefore sufficiently remote to have no effect on the cave loading. Properties of the sandstone required for the modelling were obtained from laboratory testing and from published data (Table 1); the lower values of compressive and tensile strength for the Nottingham Sandstone were used for the models.

Laboratory tests provide data on the strength of intact rock, but the caves are excavated in a fractured anisotropic rock mass, whose mass strength is lower than that of the intact rock. Input of strength data for intact rock therefore hampers creation of a realistic numerical model. A Ubiquitous Joint constitutive model was employed within the FLAC code, as this allows for the presence of orientated weakness planes within a Mohr–Coulomb solid; yield may then occur either through the matrix or along the chosen planar weaknesses, depending on the state of stress, the orientation of the weakness plane and the material properties of both the solid rock and the weak plane (Swift, 2000; Swift et al., 2000). Mechanical properties of these bedding planes were therefore required; values were taken as 80% of the matrix properties, based on laboratory tests of sandstone samples loaded parallel and perpendicular to the bedding. This input partly models the reduction in strength from the intact rock to a rock mass.

It was clear that this procedure could still not completely model the rock mass. Fractures occur in all rock masses, but there was no available data to assess a single factor by which the rock mass strength could be further reduced to simulate the real ground conditions. The full-scale test was therefore modelled numerically (Fig. 4), and its strength parameters were adjusted until its stress/deformation profile and failure mechanisms closely matched the recorded data from the real test (Swift et al., 2000). In these and other models, the boundaries were at least two cave diameters from the caves and therefore distant enough to have no influence; only the central parts of the models are shown in the figures.

The reduced strength parameters input to this successful model were then regarded as the properties of the rock mass at the test site. These represented an overall rock mass factor of 0.67 (in addition to the rock mass factor inherent to the Ubiquitous Joint Model). In practise, the reduction in strength properties was based on a non-linear Mohr envelope derived from a Rock Mass Rating, where the cohesion is reduced by a factor of 0.46, as the ratio between the original input cohesion and the cohesion value that produced the best simulation. The friction angle was similarly reduced. The rock mass properties cited in Table 1 are based on the respective intact rock properties reduced by this

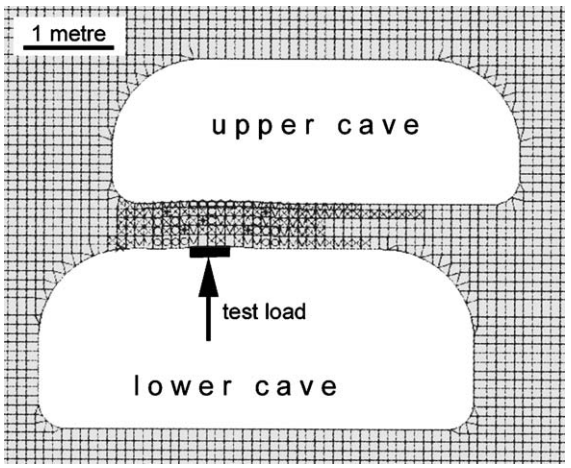

Fig. 4. Numerical model of the real cave roof test, where elements containing symbols show the initiation of complex failure in the stressed sandstone.

combined rock mass factor; these values were then used as input data for the numerical models of caves of various dimensions.

The mechanism of failure is clearly demonstrated by the numerical models. Except where a discrete bedding plane weakness had been introduced, the models showed that failure of the relatively homogeneous sandstone takes place by shear failure in a surface that encloses a plug beneath the loaded foundation (Fig. 5). The sheared plug is surrounded by a zone of opening on the ubiquitous joints, and it flares at its base where the rock fails in tension close to the cave roof. The shape of the plug and its flare are determined by the sizes and relative position of the loading pad and the cave roof.

Using strength parameters for the weaker sandstone that generally forms the roof of the more shallow caves, and the rock mass factor reduction derived from modelling the full-scale test, a series of numerical models explored the effect of different dimensions with respect to cave roof stability.

4. Physical modelling of the sandstone caves

Caves were modelled in the laboratory by excavating them to scale dimensions of 1:50 in blocks of plaster that had UCS close to 200kPa. Over a hundred models were loaded to failure. Variables covered within the test programme included cave roof thickness, cave

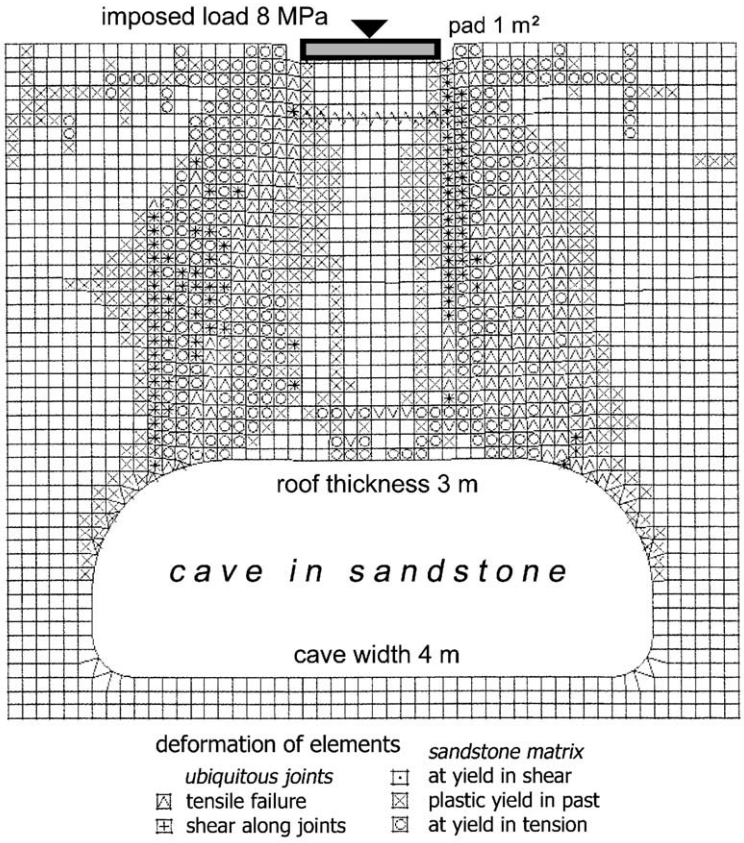

Fig. 5. Numerical model of a simple plug failure with central loading over a cave roof. The cave is 4 m wide, the roof is 3 m thick and failure stress was 8 MPa on a pad 1 m^2. The plug profile is seen in the wide zones of elements containing symbols that indicate styles of deformation or failure in shear or tension, mainly on the ubiquitous joints. The asymmetry is related to slight variation in the cave profile and the method by which the FLAC iterations proceed.

width, off-centred loading and the size and shape of the loading pad (Waltham and Chorlton, 1993). Scale factors for model cave dimensions and their appropriate plaster strength were determined by dimensional analysis (Hobbs, 1966; Lawrence, 1973); the plaster therefore represented a sandstone strength of 18 MPa.

These destructive tests clearly demonstrated the failure mechanisms (Fig. 6). Under imposed load, most cave roofs failed in plugs that developed as shear planes under the edges of the loading pad and flared towards the cave roof; these observations matched the yield data provided by the numerical models. In both physical and numerical models, asymmetrical plugs were created under loading pads that were not centred over the cave. More complex beam failures developed where individual fractures, bedding planes or lack of lateral constraint were introduced into the models.

The models demonstrated processes and indicated the relative importance of the separate variables. However, they lacked numerical realism because their cast plaster blocks lacked the small-scale bedding planes and fractures within the sandstone. Six plaster models of the real cave test were made to a linear scale of 1:25; their mean imposed load at failure, scaled up by dimensional analysis, was 11.6 MPa. The relationship of this figure to the real failure load of 2.1 MPa indicates a rock mass factor of 0.18.

Two numerical models were created to simulate the laboratory testing of the caves modelled in plaster. Strength properties of the intact plaster were determined in the laboratory, and neither the physical nor the numerical models had any internal fractures that reduced their rock mass strength. The mechanisms of failure in the numerical models match those observed in the laboratory loading tests of the plaster models, and the failure loads confirm the correlation between the numerical models, the laboratory tests on plaster models, and the full-scale loading test.

A rock mass factor rounded to 0.2 has been applied to all the physical model test results so that the homogeneous cast plaster simulates the sandstone with its planar weaknesses. The validity of this factor is confirmed by the close correlation of the adjusted data with the absolute values of failure loads indicated by the numerical modelling by FLAC.

5. Bearing capacity over the Nottingham caves

Data from all three testing programmes have been merged to provide the best assessment of the various parameters that influence foundation integrity and safe loading over the sandstone caves.

5.1. Effects of roof thickness and cave width

The single most important factor in defining the stability of a loaded foundation pad directly over a cave is the thickness of sound rock that remains to form the roof. Data from all the test programmes are combined in Fig. 7, to demonstrate the increasing loads at failure over thicker cave roofs. Loads on the physical models have been scaled up by dimensional analysis and then reduced by a rock mass factor of 0.2. Data for the numerical models are based on input

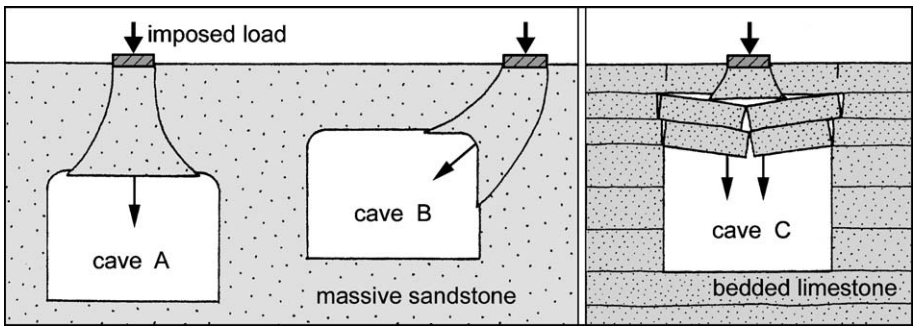

Fig. 6. Profiles of failure mechanisms observed in plaster models. In homogeneous material, the failure is a simple plug centrally over cave A, and is a curved plug from the loading pad to the offset cave B. In bedded material (with properties to model a stronger limestone) over cave C, beam failure is dominant, except for the plug failure of the upper bed in a style matched by the real cave test (see Fig. 3C).

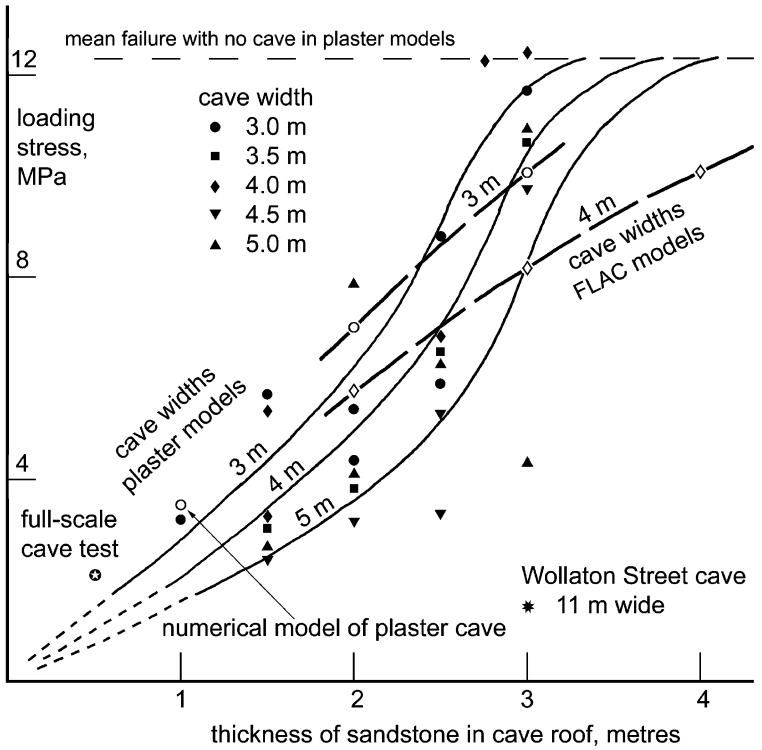

Fig. 7. Correlation between the cave roof thickness and the loading stress at failure. Data are derived from all different sources within this study, and apply to loading pads of 1 m^2 on the Nottingham sandstones. Curves are drawn for different cave widths for both the plaster model data and the numerical FLAC model data.

UCS for intact sandstone of 4.1 MPa. Correlation of the numerical and physical test data suggests that the results are realistic. All loads have been applied to a square foundation pad of 1 m^2.

The loading capacity of a typical cave roof up to 4 m wide in Nottingham Sandstone increases from about 2 MPa if it is 1 m thick to over 8 MPa if it is more than 3 m thick. Also plotted in Fig. 7 are the failure data for the tested real cave and the scaled data for a numerical model of a plaster cave; both are in sandstone of atypically high strength, and therefore plot above the main trend lines.

The width of a cave has less influence on its roof bearing capacity. The roof of a cave 5 m wide is up to 40% weaker than one that is only 3 m wide. This variation relates to the shape of the shear plug, which can flare to the width of the flat part of the roof. Curved flanks in an arched roof profile constrain any plug flare and thereby increase roof strength, but this factor remains unquantified.

The bar in Fig. 7 at 12.5 MPa is the scaled failure load on the physical models where there was no cave beneath the loading pad. This is effectively the ultimate bearing capacity of the in situ sandstone. Failure loads approach this value close to where the cave roof thicknesses equal the cave widths. The implication is that caves buried more deeply than their width are irrelevant to foundation integrity.

5.2. Effect of off-centred loading

The bearing capacity of a foundation pad is a function of its exact position relative to the boundaries of any underlying cave. Where the pad is not entirely over the cave, the failure shear plug is forced to develop a curved profile between the pad and the cave, as seen in both the physical and the numerical models (Fig. 8). The longer curved plugs have more resistance to shear, and their failure loads therefore increase significantly once the pad is at least partly

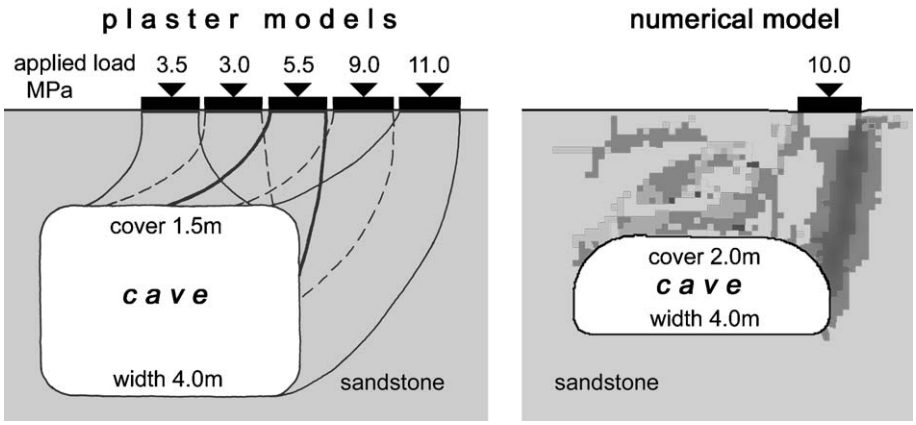

Fig. 8. Profiles of failure plugs observed in both physical and numerical models of loading pads that are not located centrally over a cave in the sandstone. Failure surfaces are drawn as observed in the plaster models, and are indicated by the darker zones of element failure in the numerical model. The higher failure load in the numerical model is due to the greater depth of its cave and also its more rounded cave profile.

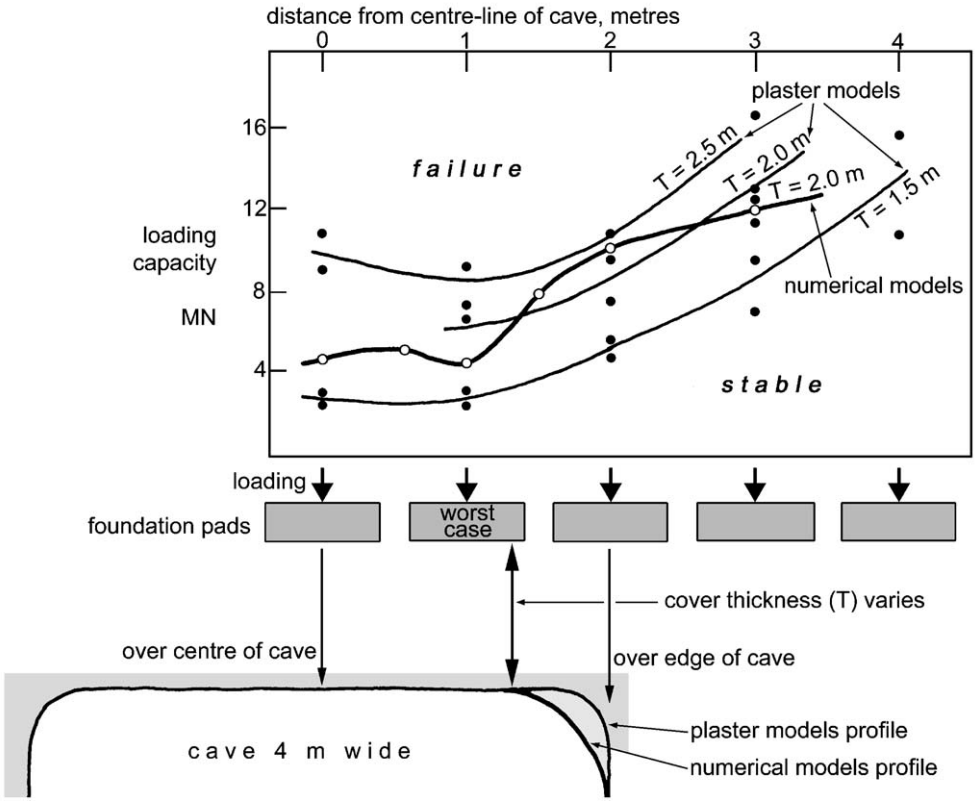

Fig. 9. Correlation between loading failure and the position of caves obliquely beneath the foundation pad, identified by both physical and numerical modelling.

above solid rock adjacent to the cave (Fig. 9). Caves that do not entirely enclose the footprint of a foundation pad have little influence on its integrity.

When the pad is entirely over the cave, the bearing capacity is largely independent of its position, as the failure is in a simple shear plug. The "worst-case" position is where a pad edge lies directly over the edge of the cave's flat roof, so that stress is concentrated in a narrow zone of shearing (Fig. 10). This situation is indicated by the dips in the graphical plots (Fig. 9), and is more exaggerated where the cave profile is less rounded.

5.3. Effects of loading pad dimensions

A square foundation pad has a larger bearing capacity whereby the total load increases in proportion to the increase of the pad's edge length. This relates directly to the development of the plug failure, whose resistance is a function of the area of the plug's shear surface, which is almost directly related to the plug or foundation pad's perimeter.

A limited series of laboratory tests on plaster models indicated how long stiff strip foundations can bridge over caves. Bearing capacities increased greatly when the strip length was increased beyond 1–2 m greater than the cave length, so that it gained support equivalent to that from pad foundations on each side of the cave.

6. Highway loading of a very wide cave

A cave with a maximum width of 11 m was found underneath Wollaton Street, the trunk road entry to Nottingham's city centre from the west (Fig. 11). It has a sandstone roof less than 3 m thick, and is by far the widest cave that has not already collapsed in the city. Though the cave has survived beneath the road for more than 100 years, there was concern for its stability after a large slab fell away from the roof span early in 1997 (and prompted the owner to contact the city's highway engineers, who had not previously known of the cave). The site was surveyed (Fig. 12) and the cave roof profile was analysed by reference to design codes for masonry arches. Intact strength of the sandstone was measured on some of the fallen blocks, but a rock mass factor had to be estimated. Factors of safety were derived for a sensible range of values, and were found to be between 2 and 5. With no better data then available, a load-bearing wall was built down the centre of the cave in order to halve the unsupported span (Waltham and Cubby, 1997).

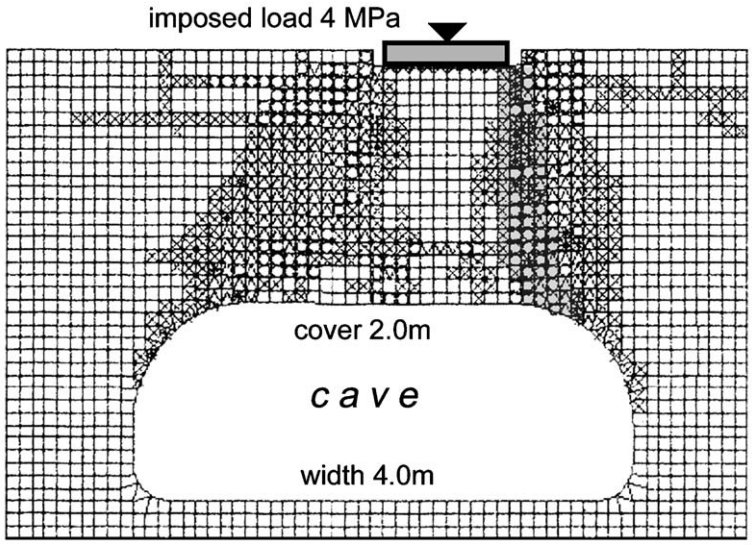

Fig. 10. The worst-case position for a loaded pad with the edge of its footprint over the edge of the flat roof of a cave, so that shear failure on one side of the plug is concentrated in a short narrow zone.

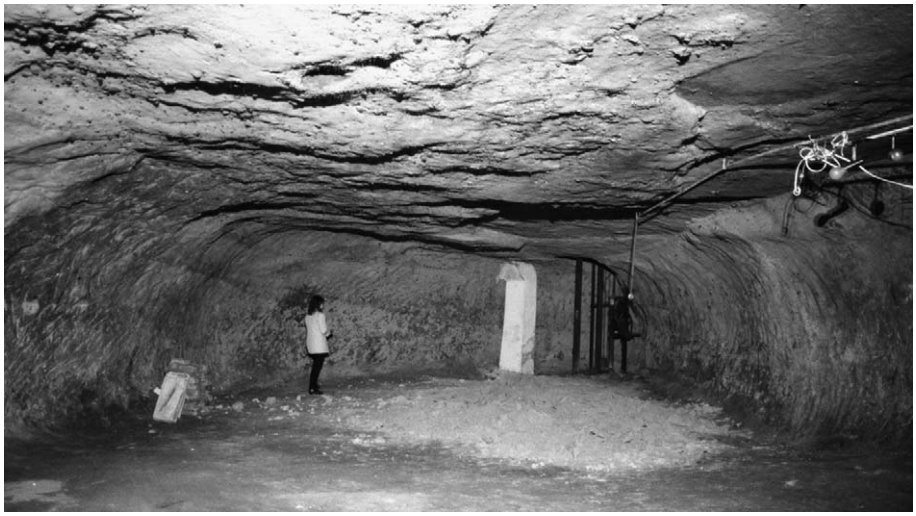

Fig. 11. The wide cave in sandstone beneath Wollaton Street, before the central support wall was built within it. The light coloured debris on the floor is the remains of the bedding slab that had just fallen from the slightly darker recess in the roof.

Subsequently, the widest profile of the Wollaton Street cave was modelled numerically. Strength parameters of the sandstone were initially taken from laboratory tests on samples from the roof fall (Table 1). The gently dipping bedding plane that delimited the recent roof fall is a smooth surface, partly marked by a very thin clay parting and having negligible tensile strength; this was simulated in the model, in addition

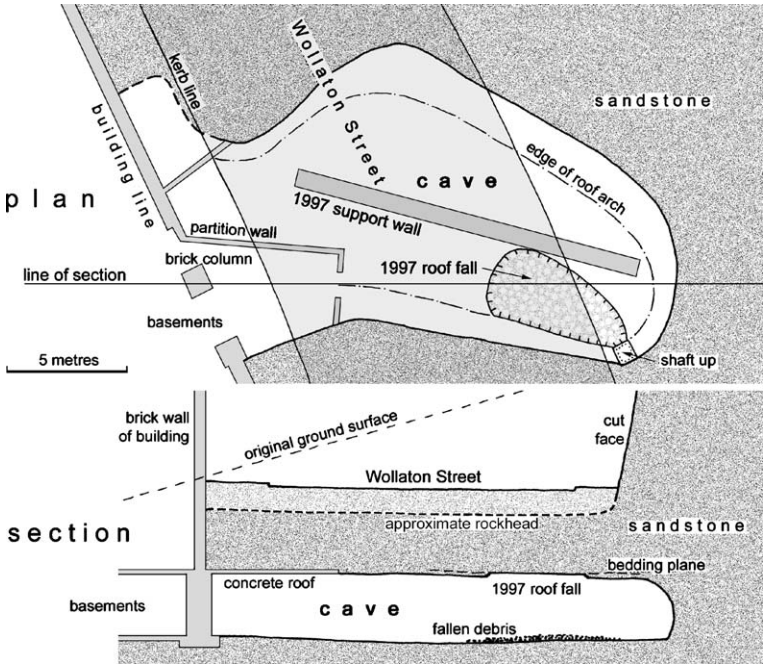

Fig. 12. Outline plan and profile of the cave beneath Wollaton Street. The support wall within the cave was built shortly after the adjacent roof fall occurred.

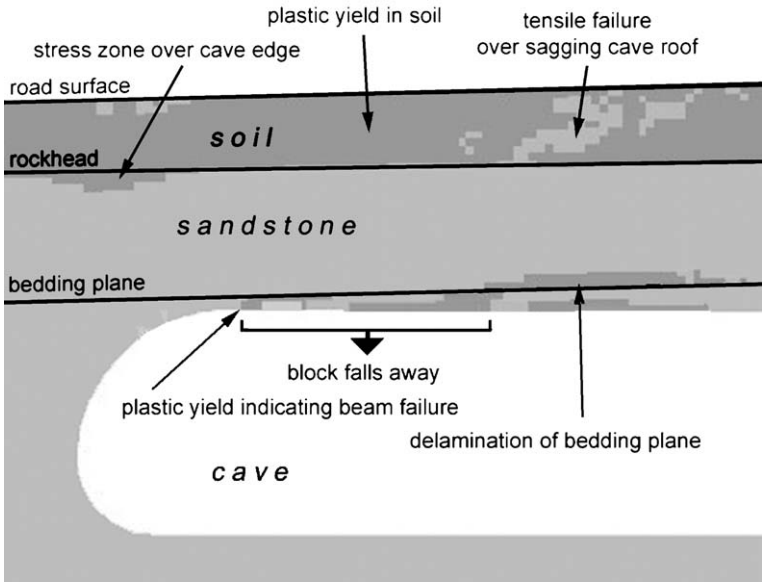

Fig. 13. Plastic state of elements above the left half of the Wollaton Street cave, showing zones of yield in shear (dark) within the sandstone matrix, under self-load alone. This model also shows de-lamination of the bedding plane, indicating the portion of the roof that has failed.

to the bedding planes defined in the Ubiquitous Joint Model. The fill between the rockhead and the road surface was assigned nil cohesion and a friction angle of 45°. Within the numerical models, instability is determined by monitoring the history of vertical displacement at various locations in the roof. Once displacements decline to zero under increasing load, the ground is considered to be stable. Conversely, accelerating displacements indicate failure.

Initially, the stability of the cave roof was assessed under the load of self-weight alone, with no imposed load. This model indicated that failure of the entire roof structure would occur. Since the cave is still largely intact, this model underestimated the strength of the rock mass, though the real cave could have gained some modest extra support by its wall profile in the third dimension It was based on strength parameters derived from tests on fallen blocks of sandstone within the failed slab, and these may not be truly representative of the intact rock mass if they had suffered from impact loading in their fall. In subsequent models, the strength parameters were taken as those of other samples of the Nottingham Sandstone (Table 1).

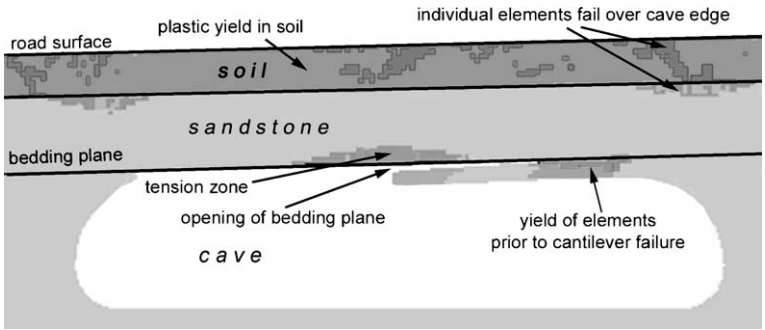

Fig. 14. Failure zones (dark) within the sandstone bed remaining beneath the bedding plane, after the adjacent roof failure in the Wollaton Street cave with no internal support.

In a second model, the stability of the cave roof was again assessed without imposed load. This showed that the initial beam failure would have occurred under self-weight alone, and indicates that the mode of failure may have been one of continual creep with de-lamination of the gently dipping bedding plane above the roof bed. The model also shows that the remaining part of that bed would not have collapsed under self-loading alone (Fig. 13).

A subsequent model examined the behaviour of the cave under highway loading. In line with highway design procedures, a constant load of 17 kPa was applied over the entire upper surface of the model (representing the road surface) with an additional constant load of 33 kPa applied on a 1 m^2 pad at the surface above the centre-line of the cave. The new model was run until the initial beam failure occurred, was re-run under the prescribed loading conditions after the failed beam was removed, and was also re-run with the support wall in place to assess the wall's role in long-term stability. This indicates that, under highway loading conditions and without any internal support wall, the bed of sandstone remaining after the initial fall collapses beneath the bedding plane (Fig. 14). It also shows that failure of this small portion of the sandstone bed does not lead to catastrophic failure of the overall roof, and the risk of surface instability under highway loading conditions is therefore low.

The point load at the surface required to induce catastrophic failure in the remaining sandstone beam above the bedding plane was found to be 400 kPa (applied to a pad of 1 m^2 over the centre of the cave).

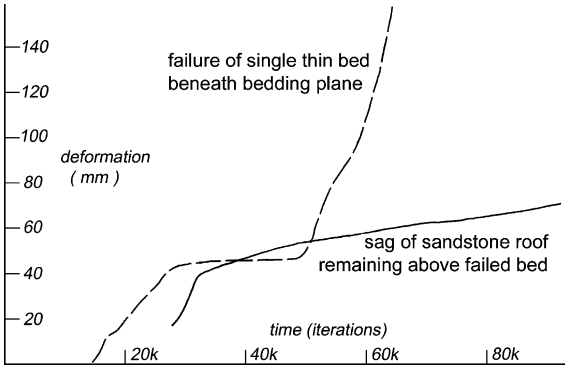

Fig. 16. Vertical displacement against time (as iterations) for points over the centre of the Wollaton Street cave. The solid line shows slow creep of the roof rock above the failed beam, under highway loading, indicating that it remains in place and the roof is not continuing to fail in a stoping mechanism that may lead directly to a crown hole failure. The broken line shows the total failure (under a high point load) of the beam adjacent to an installed support wall.

This value is low in comparison to the failure loads recorded for other cave profiles–but this is an unusually wide cave with an unsupported span of 11 m, located at a shallow depth in a relatively weak sandstone. The model reveals the failure mechanisms for the beam that constitutes the entire sandstone roof of the cave, after the rock has fallen away from below the major bedding plane (Fig. 15). There are zones of plastic yield within the sandstone (both in shear along the bedding planes and in tension across the ubiquitous joints) above each shoulder of the cave, indicating that failure in these zones is ultimately controlled by the shear strength of the rock matrix. In addition,

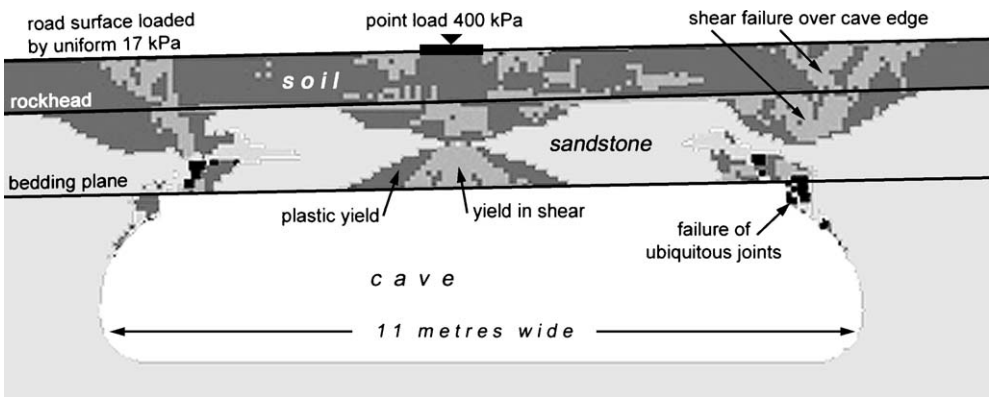

Fig. 15. Deformation zones in the ground around the Wollaton Street cave. The darker tones indicate zones of yield within the matrix of both the soil and the sandstone as labelled.

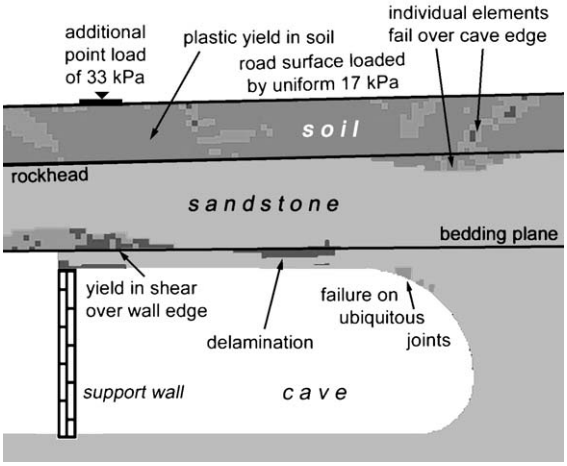

Fig. 17. Plasticity indicators around the Wollaton Street cave under highway loading and after installation of the internal support wall. There is a spread load of 17 kPa across the entire ground surface, and an additional point load of 33 kPa applied to a square of 1 m^2 at the worst-case site over the edge of the support wall.

there is a large zone above the centre-line of the cave where shear and tensile yield indicate that failure is also controlled by the strength of the rock matrix. Localised sites of yield along (shear) and across (tensile) bedding planes are also present above this zone.

The history of displacement recorded during this failure, for a point above the centre-line of the cave, indicates only a gradual vertical movement of the sandstone into the void (Fig. 16). This is in contrast to the post-yield behaviour under higher imposed loads, where the collapse takes place much more rapidly. The slow failure of the roof under highway loading indicates that any ground collapse should be preceded by small (but recognisable) movements, which would give sufficient time to take preventative engineering action.

6.1. Internal support for a cave roof

A subsequent numerical model of the Wollaton Street cave then had the fallen part of the roof bed (the initial, observed rock fall) removed and the load-bearing wall added. The point load (on the 1 m^2 pad) was then applied at the ''worst-case'' location, immediately adjacent to the wall, so that failure occurred where shear stress was concentrated within the shortest zone.

Under the same highway loading conditions (with 17 kPa applied to the whole road and 33 kPa applied on a 1 m^2 pad), the built wall provides sufficient support to the surviving part of the roof bed beneath the bedding plane to prevent collapse in to the cave. Although areas of shear and tension can be seen above the shoulder of the cave, displacements in this part of the beam, and in the overlying rock beam, converge to zero over time, indicating that a static equilibrium is achieved (Fig. 17).

This model was then run with increasing load on a pad 1 m^2 in the worst-case site (immediately adjacent to vertically above the wall) to determine the load at which the roof would fail when supported by the wall. This model indicates a failure load of 600 kPa on the pad (Fig. 18), and also that the overlying sandstone beam would also fail at this load. This

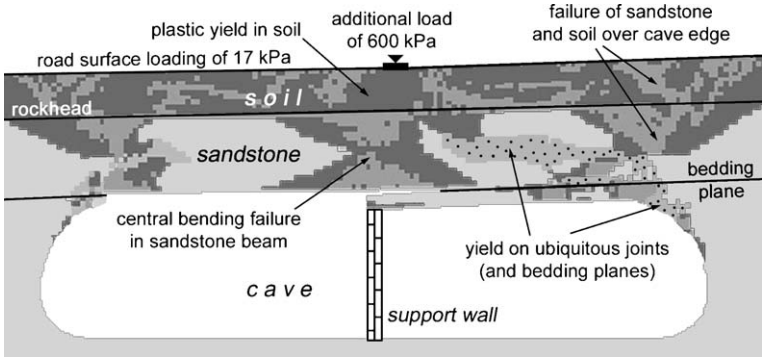

Fig. 18. Deformation zones within the entire roof above the Wollaton Street cave after installation of the internal support wall, and at the point of failure induced when loading on the single pad (1 m^2) was increased to 600 kPa.

could have serious consequences for the road above the cave, but the bearing capacity appears to be a 50% improvement on the load capacity of the unsupported roof. Although there is extensive plastic yield within the rock shoulder of the cave, it appears that failure is also induced lower down in the cave wall. Plastic yield is observed immediately adjacent to the cave shoulder but does not extend through the total thickness of the lower sandstone roof bed; this indicates that beam failure is incomplete in this area. The model shows that the bedding plane opens above the sandstone beam, but this is due to deformation of the supporting wall, whose strength appears to be underestimated and was not investigated further in this study.

7. Implications for construction on cavernous ground

For safe construction, there is a critical cover thickness that makes an underlying cave irrelevant to imposed loading. Sound engineering should therefore follow a ground investigation that finds any cave within the hazard zone at any lesser depth.

7.1. Building regulations in Nottingham

Current building regulations within the city demand that solid ground is proven beneath all planned foundations to a depth of 3 m where loading is <300 kN and to 5 m for greater loading. The investigation depth required varies with the structural load, but makes no reference to pad size. This study suggests (Fig. 7) that these requirements are more than adequate, and that some err on the side of safety. For loading at the locally accepted Safe Bearing Pressure (SBP) for the Sherwood Sandstone, of 1 MPa, the factor of safety over caves that satisfy these regulations is 8 or more. This may be appropriate in rock where structural detail can neither be ascertained nor be quantified meaningfully. The required thicknesses of rock cover provide reasonable but not complete protection against crown hole development (Waltham, 1993). Though crown hole failures through more than 3 m of sandstone are unknown in Nottingham, they could occur theoretically, but the best defence against them is proper control of water and drainage including the prevention of all leakages.

Relationships between cave width, roof thickness and failure loads are shown in Fig. 19, and the choice

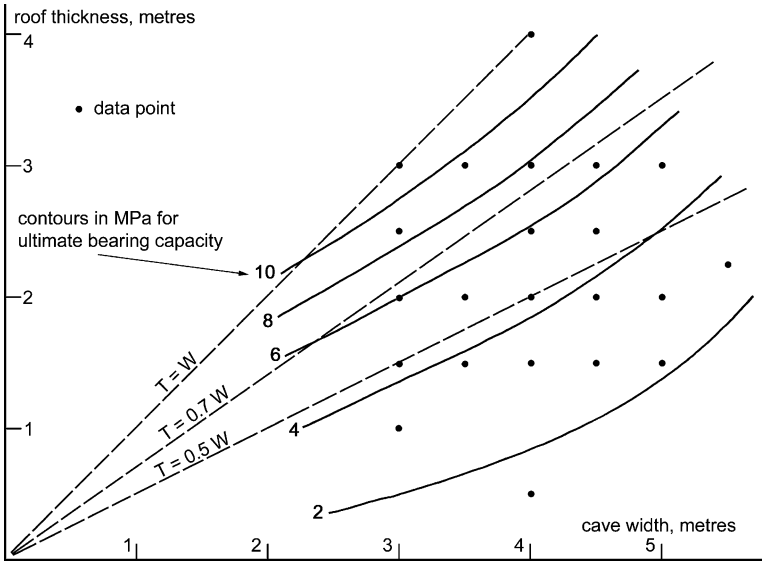

Fig. 19. Ultimate bearing capacities over cavities of variable width and roof thickness within the Nottingham Sandstone. The broken lines show values for guidelines that are based on various ratios of roof thickness (T) to cave width (W). Contours are based on 30 data points (some superimposed); the Wollaton Street cave plots off the graph to the right.

of a guideline relating safe cover thickness to cave width is dependant on the factor of safety required. Even the least conservative guideline, demanding cover that exceeds half the cave width, appears to be adequate where structural loading that is less than the locally applied SBP of 1 MPa. Where a cave is found with a rock cover in the range of 3–5 m, the narrower caves pose no hazard to normal construction works, and a cover thickness of 5 m is only required over caves significantly wider than those that are typical beneath Nottingham. More concern should be expressed over the weathering state of the sandstone, as some caves can exist in highly weathered sandstone that is significantly weaker than the typical rock beneath the city.

Boreholes raked out from the foundation footprint, as required by Nottingham's building regulations, are inappropriate. Caves provide a significant hazard only where they underlie the entire footprint of a foundation pad, and provide no hazard at all where they are laterally offset. Vertical boreholes will reveal any hazardous cave, while caves found only in raked boreholes may cause unwarranted concern and delays to construction projects.

7.2. Implications for cavities in other rocks

Even though the stability of mine roofs and of mine pillars are well understood, there is a shortage of experimental data on structural loading over ground cavities. At shallow depth, the Nottingham Sandstone is a weak rock (UCS = 5 MPa) with a low mass strength (RMR = 30–40), yet caves within it are still stable under load where cover thickness exceeds cave width. This suggests that the simple guideline is conservative in stronger rocks.

Most karstic limestones that contain large natural caves are much stronger (UCS = 50–100 MPa, RMR = 40–60). Quantification of their rock mass properties is almost impossible, and test data is lacking. Numerical modelling of the Nottingham caves with a stronger sandstone showed that bearing capacity increased directly with strength. This suggests that an engineering guideline that cover thickness should exceed 50% of cave width would appear to be reasonable for most construction projects on typical karstic limestone. A safe bearing pressure of 4 MPa is sometimes used for design on strong limestone. Where these higher loads are to be imposed, a guideline that cover should exceed 70% of cave width, is more appropriate as a starting point for an unknown site. For a limestone with double the mass strength of the Nottingham Sandstone, this would provide a factor of safety of about 3.5 (Fig. 19). The old rule-of-thumb that cover should exceed width appears to be unjustified in typical cavernous limestone.

Many structures do stand on rock that is far thinner than in these ratios. However, such guidelines would not apply to chalks and weaker limestones with mass properties more comparable to the Nottingham sandstone. They would also not apply to old coal mines where cavity migration in weak shale roof material can make very small mines a hazard at considerable original depth. For caves and voids in stronger rocks, site-specific investigation is warranted, in which case acceptable ratios of cover over cavities may be modified where the rock mass is demonstrated to be of good quality.

Acknowledgements

The authors gratefully acknowledge the support of many colleagues at their two universities who have contributed to the modelling and testing of Nottingham's caves. For work on the cave test loading, we thank Alan Freebury and the technicians of the Civil Engineering Department at Nottingham Trent University. For assistance with the numerical testing, we thank Dave Reddish and Phil Lloyd at Nottingham University, and Hui Chen, David Johnson, Mike Rosenbaum and Ali Roodbaraky at Nottingham Trent. For most of the physical modelling, we thank Chris Holland, Ian Maplethorpe, Ian Froggatt, Zoe Lonsdale, Ian Crosby, Ian Chorlton, Richard Storm and others at Nottingham Trent who carried out the laboratory testing for their undergraduate projects.

References

Forster, A., 1989. Engineering geology of the Nottingham area. British Geological Survey Technical Report, WN/89/4.

Hobbs, D.W., 1966. Scale model studies of strata movement around mine roadways: apparatus, techniques and some preliminary

results. International Journal of Rock Mechanics and Mining Sciences 3, 101–127.

Itasca, 1995. Fast Lagrangian Analysis of Continua (FLAC). Version 3.3. Itasca Consulting Group, Minneapolis, MN.

Lawrence, D., 1973. Scale model studies of strata movement around mine roadways: VII. Effects of horizontal and vertical pressure. International Journal of Rock Mechanics and Mining Sciences 10, 173–182.

Roodbaraky, K., Chen, H., Waltham, A.C., Johnson, D., 1994. Finite element analysis of the failure of a sandstone cave roof in Nottingham. In: Proceedings of 3rd European Conference on Numerical Methods in Geotechnical Engineering. Balkema, Rotterdam, pp. 409–416.

Swift, G.M., 2000. An examination of stability issues relating to abandoned underground mine workings. PhD thesis, Nottingham University.

Swift, G.M., Lloyd, P.W., Reddish, D.J., Waltham, A.C., Rosenbaum, M.S., 2000. Numerical modelling of rock loaded to failure above underground cavities. Proceedings GeoEng2000. Melbourne, vol. 2, p. 184.

Walsby, J.C., Lowe, D.J., Forster, A., 1990. The caves of the city of Nottingham: their geology, history, extent and implications for engineers and planners. In: Cripps, J.C., et al. (Eds.), Engineering Geology of Weak Rock. Balkema, Rotterdam, pp. 481–488.

Waltham, A.C., 1992. The sandstone caves of Nottingham. Mercian Geologist 13, 5–36.

Waltham, A.C., 1993. Crown hole development in the sandstone caves of Nottingham. Quarterly Journal of Engineering Geology 26, 243–251.

Waltham, A.C., Chorlton, I.G., 1993. Rock roof stability in the sandstone caves of Nottingham. In: Cripps, J.C., et al. (Eds.), Engineering Geology of Weak Rock. Balkema, Rotterdam, pp. 489–492.

Waltham, A.C., Cubby, T.J., 1997. Developments in Nottingham's sandstone caves. Mercian Geologist 14, 58–67.